Military Technical College
Kobry El-Kobbah,
Cairo, Egypt.

17th International Conference on Applied Mechanics and Mechanical Engineering.

NUMERICAL STUDY OF TRANSFER PROCESSES IN SWEEPING GAS MEMBRANE WATER DISTILLATION

A. A. Aboulkasem*, M. S. Hassan*, A. G. Ibrahim* and S. El-Shamarka*

ABSTRACT

In this research, the water transport through nanoporous membranes was predicted by developing a two-dimensional model. A simulation for sweeping gas membrane distillation (SGMD) process was carried out using computational fluid dynamics. The developed model consists of a nanoporous flat-sheet membrane and saline water as a feed on one side. A stream of air is blown as a vapor collector on the other side aiming at investigation of the factors affecting the air humidification process. The model uses the basic equations of momentum, heat, and mass balance. First, pure water was used as a permeate fluid and the simulation results was verified by comparing it with the data reported in literature showing good agreement. Second, the stream of air replaced the side of pure water. Diffusion of water through the membrane pores was simulated by combination of Knudsen flow, and molecular diffusion. The simulation results stated that the operation conditions such as fluids temperatures and velocity beside the membrane characteristics affect both the amount of water transported through the membrane pores and the moisture-enthalpy ratio.

KEYWORDS

Mass transfer, humidification, membrane distillation, SGMD, COMSOL Multiphysics®.

* Egyptian Armed Forces.

NOMENCLATURE

A	membrane surface area (m^2)
a_w	water activity in NaCl solution
atm	atmospheric
B	Membrane distillation coefficient ($kg/(m^2.s.Pa)$)
c	concentration (mol/m^3)
C_p	heat capacity at constant pressure (J/(kg K))
D_K	Knudsen diffusion coefficient (m^2/s)
D_t	total diffusion coefficient (m^2/s)
D_{wa}	molecular diffusion coefficient of water into air (m^2/s)
d_p	pore diameter (m)
h	specific enthalpy (kJ/kg)
Kn	Knudsen number (-)
k	thermal conductivity (W/(m K))
M	molecular weight (kg/mol)
m	molality of NaCl in NaCl solution
$\dot{m}$	mass flow rate (kg/s)
N	molecular flux ($kg/(m^2.s)$)
P	total pressure (Pa)
ΔP_v	transmembrane vapor pressure difference (Pa)
P_0	vapor pressure of pure water (Pa)
P_i	actual vapor pressure of saline water (Pa)
R	gas constant (J/(mol K))
s	NaCl concentration (g/kg water)
T	temperature (K)
u	velocity component in x-direction (m/s)
v	velocity component in y-direction (m/s)
W	humidity ratio (g water vapor/kg dry air)

Greek letters

ε	membrane porosity (-)
μ	viscosity (Pa s)
ρ	fluid density (kg/m3)
τ	membrane tortuosity factor (-)
δ	membrane thickness (m)

Subscripts

a	air
eff	effective
g	gas inside the membrane
in	inlet
m	membrane
ma	membrane-air interface
mw	membrane-water interface
NaCl	sodium chloride
out	outlet
s	solid membrane
w	water

INTRODUCTION

Since about two decades, membrane processes showed great potential to replace conventional energetically intensive techniques of water purification such as distillation and evaporation, to accomplish the selective and efficient transport of specific components [1].

In the field of desalination, membrane-based reverse osmosis (RO), thermal-based multi-stage flash (MSF), and multi-effect distillation (MED) constitute over 90% of the global desalination capacity. RO plants, with typical capacities of ~20000 m^3 d^{-1}, account for ~41% of the total desalination capacity while MSF plants, with typical capacities of ~76 000 m^3 d^{-1}, account for ~44% [2].

Recently, membrane technology is highlighted in water desalination by distillation being investigated as energy saving alternative. The membranes used in membrane distillation (MD) must be porous and hydrophobic. Mostly, the vapor pressure characteristics of water controls pressure gradient across the membrane [3].

As the interface between the air and water is presented through a media, the concept of “effective area” is the direct air-water contact area. In the case of porous membrane at the interface, the effective area can be considered as the total of the inside area of the pores. One can imagine what an enormous area is generated here if it is stated that the density of the pores is in order of $10^8/cm^2$. Naturally, this density is inversely proportional to the pore size.

Transport of water between two phases in MD can be accomplished by different methods due to the technique creating low pressure at permeate side. Various MD processes including direct-contact membrane distillation (DCMD), air-gap membrane distillation (AGMD), vacuum membrane distillation (VMD), and sweeping gas membrane distillation (SGMD) are considered [4].

Among various types of MD, the SGMD is the rarely studied MD configuration. Only 4.5% of the MD papers published up to December 2010 in refereed journals deal with SGMD technology [5], where inert gas is used to sweep the vapor at the permeate membrane side to condense outside the membrane module. There is a gas barrier, like in AGMD, to reduce the heat loss, but this is not stationary, which enhances the mass transfer coefficient [4]. However, SGMD configuration has a great perspective for the future because it combines a relatively low conductive heat loss through the membrane with a reduced mass transfer resistance [5].

SGMD involves: (a) the evaporation of water at the hot feed side; (b) transport of water vapor through dry pores of hydrophobic membranes due to transmembrane vapor pressure, which is the driving force; (c) collection of the permeating water vapor by an inert cold sweeping gas; and (d) condensation out of the membrane module. The membrane acts only as a support for a vapor-liquid interface and does not contribute to the separation mechanism [6].

Modeling and simulation of SGMD could be useful for understanding transport mechanism. However, modeling of transport phenomena in SGMD is difficult and complicated because both mass and heat transfer must be taken into account [7].

Recently, computational fluid dynamics (CFD) simulation of membrane processes has been studied [8-11] showing that CFD is a powerful tool for simulation of membrane contactors.

The aim of the current study is to predict the effect of air and water temperatures, air velocity, and membrane characteristics on both the molecular flux through the membrane and the moisture-enthalpy ratio. A 2-D configuration of SGMD in a flat-sheet module is used. The basic equations including momentum, heat, and mass transfer are solved using CFD techniques.

MODELING

In the beginning, a mathematical model which accounts all transport phenomena in the process is considered to reproduce a DCMD model already published in literature [7, 12]. In this model, the transport equations include energy convection and conduction for the feed and the permeate channel, conduction for the membrane layer, momentum transport for the feed and the permeate channels, and mass transport for the membrane pores. A combination of Knudsen/Poiseuille flow was used.

As it is illustrated in Fig.1, the feed solution which is a hot saline water is passed through one side of membrane contactor, and the cold water is flown counter-currently in the permeate side. The water is evaporated at the feed–membrane interface and then is transported through the pores of membrane. Temperature difference between two phases is the driving force for transport of water.

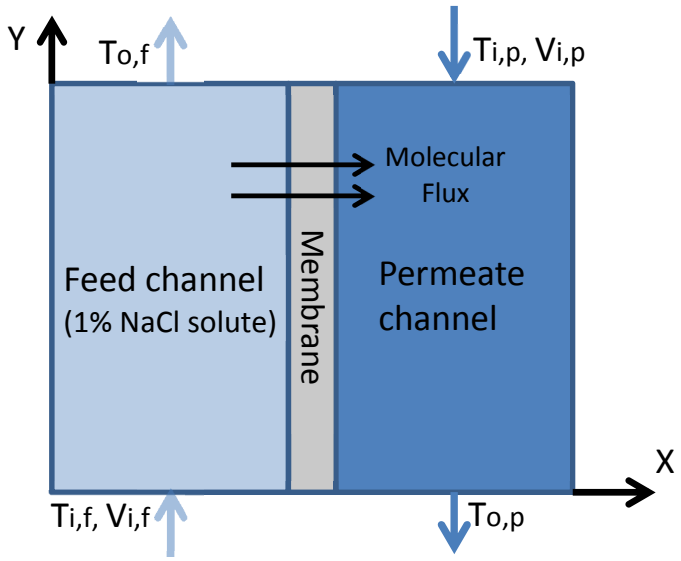

Figure 1. Schematic of the model used in simulation of DCMD.

After transport through the membrane pores, water vapor is then condensed in the cold side. The comparison between the published model results and the reproduced one are illustrated in appendix A. After the verity of the reproduced model has been confirmed, a modified one was developed for simulating SGMD process.

The modified model for the present study is shown in Fig. 2. Now the momentum transport is considered only for the air channel, which considered as a moist air domain while the water is stagnant. A combination of Knudsen flow and molecular diffusion is considered for the mass transport. The geometry and nominal conditions in the study are as follows:

a) Air inlet boundary (B–D) and air outlet boundary (A–C): 30 mm
b) Membrane thickness (C-E): 1 mm
c) Lower vessel depth (E-G): 50 mm
d) Membrane length for transportation process (E–F) and (C–D): 100 mm
e) Air velocity 0.5 m/s; porosity 0.83; tortuosity 1.1; mean pore size 220 nm; total pressure 1 atm.; seawater temperature 60^{0}C; inlet air temperature 20^{0}C; relative humidity of air channel 100%. One or more characteristics may be changed to reflect the system responses to these changes, but the others are kept unchanged.

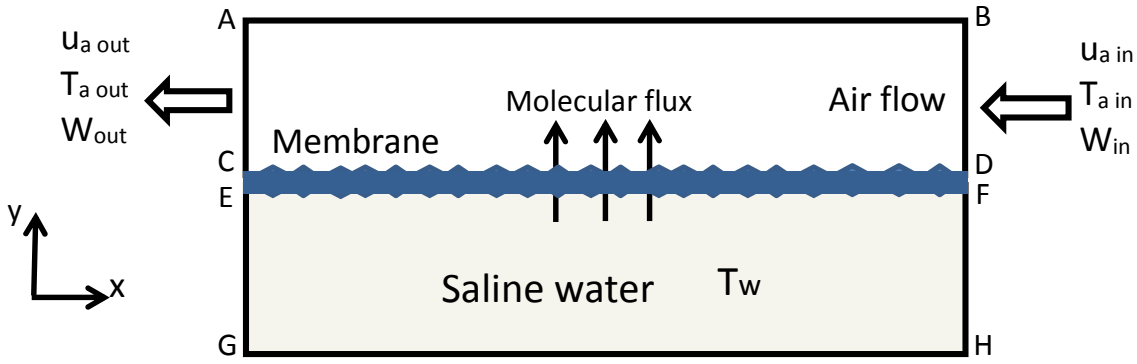

Figure 2. Schematic of the model used in simulation of the present 2-D SGMD study.

Governing Equations

Momentum

For the air channel, the incompressible Navier-Stokes equations were used for momentum balance in terms of air pressure and velocity vector of in x-direction:

$$\rho_a \left[u_a \left(\frac{\partial u}{\partial x}\right) + v_a \left(\frac{\partial u}{\partial y}\right)\right] = -\frac{\partial}{\partial x} P + \mu_a \left(\frac{\partial^2 u}{\partial x^2} + \frac{\partial^2 u}{\partial y^2}\right) \quad (1)$$

$$\left[\left(\frac{\partial u}{\partial x}\right) + \left(\frac{\partial u}{\partial y}\right)\right]_a = 0 \quad (2)$$

where ρ_a and μ_a are the density and dynamic viscosity of air, respectively.

Heat transfer

For seawater side, the temperature is considered constant all over the domain.

For air side, heat is transferred by convection and conduction mechanisms and the energy balance can be derived in terms of temperature and velocity vector of air in x-direction as:

$$\rho_a \, C_{pa} \, u_a \frac{\partial T_a}{\partial x} - k_a \left(\frac{\partial^2 T_a}{\partial x^2} + \frac{\partial^2 T_a}{\partial y^2}\right) = 0 \qquad (3)$$

where ρ_a, C_{pa}, and k_a are the density (kg/m^3), specific heat capacity at constant pressure (J/(kg.K)), and thermal conductivity (W/(m.K)) of air, respectively.

For membrane layer, heat is transferred by conduction mechanism and derived in terms of the temperature inside the membrane:

$$\nabla \cdot (k_m \nabla T_m) = 0 \qquad (4)$$

$$\frac{\partial}{\partial x}\left(k_m \frac{\partial T_m}{\partial x}\right) + \frac{\partial}{\partial y}\left(k_m \frac{\partial T_m}{\partial y}\right) = 0 \qquad (5)$$

where k_m is the thermal conductivity (W/(m.K)) of the membrane matrix.

$$k_m = \varepsilon \cdot k_g + (1 - \varepsilon) k_s \qquad [12, 13] \qquad (6)$$

where ε is the membrane porosity, k_g and k_s refer to the thermal conductivity of vapor within the membrane pore and the solid membrane, respectively.

The thermal conductivity of the gas phase in the pores of membrane can be written as [13]:

$$k_g = 0.0144 - 2.16 \times 10{-}5(T_m) + 1.32 \times 10{-}7(T_m)^2 \qquad (7)$$

where T_m is the temperature inside the membrane [K].

Mass transfer

Transport of water vapor through the membrane is modeled by solving concentration equation. Concentration equation is a simplified form of continuity equation, which only considers diffusional mass transfer, and may be expressed as:

$$\nabla \cdot (-D_t \nabla c) = 0 \qquad (8)$$

$$\frac{\partial}{\partial x}\left(-D_t \frac{\partial c}{\partial x}\right) + \frac{\partial}{\partial y}\left(-D_t \frac{\partial c}{\partial y}\right) = 0 \qquad (9)$$

where c denotes the concentration of water vapor (mol/m^3) and D_t denotes the total diffusion coefficient (m^2/s).

For membranes with air filled pores having pore sizes smaller than 0.5 μm (which is our case), the molecule–pore wall collisions begin to occur as frequently as the

molecule–molecule collisions [14]. M. Khayet et. al. [15] proved that the combined Knudsen–molecular diffusion is the most adequate for SGMD process. So, it will be considered as being responsible for the water transport through the membrane. The latter combined diffusion coefficient may be obtained from the equation [16]:

$$D_t = [(D_{K\,eff})^{-1} + (D_{wa\,eff})^{-1}]^{-1} \quad (10)$$

where $D_{K\,eff}$ represents effective Knudsen diffusion (m^2/s) and $D_{wa\,eff}$ represents effective molecular diffusion of water vapor into air through the porous membrane (m^2/s) which may be written as [15, 16]:

$$D_{K\,eff} = \frac{\varepsilon}{\tau} (d_p/3) (8RT_m/\pi M_w)^{0.5} \quad (11)$$

where ε, τ, d_p, R, M_w denote porosity (-), tortuosity (-), mean pore diameter (m), gas constant (8.3144 J/(mol.K)), and molecular weight of water (0.018 kg/mol) respectively. It should be noted that the term $(8RT_m/\pi M_w)^{0.5}$ can be referred as mean molecular speed (m/s).

D_K can be simplified further as Eq. (12) [12, 16]:

$$D_{K\,eff} = \frac{\varepsilon}{\tau} 4850\, d_p\, (T_m/M_w)^{0.5} \quad (12)$$

In Eq. (12), d_p has the unit of cm, M_w has the unit of g/mol, temperature T_m has the unit of K, and D_K has the units of cm^2/s.

$$D_{wa\,eff} = \frac{\varepsilon}{\tau} D_{wa} \quad (13)$$

where D_{wa} represents molecular diffusion coefficient of water vapor into air (m^2/s) which can be estimated in terms of temperature and pressure [4]:

$$PD_{wa} = 1.895\times10^{-5}\, T_m^{2.072} \quad (14)$$

where P is the total pressure (Pa), D_{wa} in (m^2/s), and T_m in (K).

It is worth here noting that the key factor to define the mass transport mechanism is Knudsen number (Kn) which can be defined as the ratio of the mean free path of transported molecules to the membrane pore size. The mean free path value of water vapor at 60 ^{0}C was estimated by Al-obidni et al. [17] to be 0.11 µm.

Heat and mass transfer coupling

As mentioned, the temperature difference gives rise to a water-vapor pressure difference and, consequently, to a transmembrane molecular flux (N). The MD molecular flux, *N*, can be written as a function of the transmembrane water-vapor pressure difference, ΔP_v [4, 6, 12]:

$$N = B\ \Delta P_v \tag{15}$$

where B is MD coefficients (kg/(m2.s.Pa)). This coefficient depends on membrane characteristics (thickness, tortuosity, etc.), as well as on different experimental parameters (temperature, pressure, etc.).

According to the Knudsen/molecular diffusion mechanism, the MD coefficient may be written as [6, 15]:

$$B = (M_w/RT_m\boldsymbol{\delta})\ D_t \tag{16}$$

and

$$\Delta P_v = P_{v,\,mw} - P_{v,\,ma} \tag{17}$$

The water-vapor pressure at the water side of the membrane, $P_{v,\,mw}$, can be written with the Antoine equation [18]:

$$P_{v,\,mw} = \exp\,(23.5377 - 4016.36/\,(T_{mw}\text{-}38.63)) \tag{18}$$

where $P_{v,\,mw}$ is the vapor pressure of pure water (Pa) and T is the temperature (K). However, when real solutions are used as feed, the water vapor pressure on the feed side is lowered due to the reduced water activity [14, 18]. The actual vapor pressure P_i can be recalculated using the activity a_w:

$$P_i = P_{v,\,mw}\ a_w \tag{19}$$

The water activity can be estimated by the equation [18]:

$$a_w = 1 - 0.03112\ m - 0.001482\ m^2 \tag{20}$$

where m is the NaCl molality (mol NaCl per kilogram pure water).

$$m = s\ /\ M_{NaCl} \tag{21}$$

where s is NaCl concentration (g/kg water), M_{NaCl} is the molecular weight of NaCl (=58.44 g/mol).

On the other side, The water-vapor pressure at the air side of the membrane, $P_{v,\,ma}$, can be written as a function of the total pressure, P (Pa), and the humidity ratio, W:

$$P_{v,\,ma} = \frac{(W/1000)P}{\left(\frac{W}{1000}\right)+0.622} \tag{22}$$

The humidity ratio along the membrane module length may be related with the air mass flow rate, $\dot{m}_a$ (kg/s), and with the humidity at the membrane module inlet, W_{in} [6, 15]:

$$W = W_{in} + \frac{NA}{\dot{m}a} \tag{23}$$

where A is the membrane surface area (m^2). Now, Eqs. (15), (17), (22) and (23) permit writing a second-grade equation for the SGMD flux as follows:

$$N^2 + q_1 N + q_2 = 0 \tag{24}$$

where the coefficients q_1 and q_2 are given by:

$$q_1 = [(\dot{m}_a/A)(W_{in}+0.622) + B(P-P_{v,\,mw})] \tag{25}$$

$$q_2 = B(\dot{m}_a/A)\,[PW_{in} - P_{v,\,mw}(W_{in}+0.622)] \tag{26}$$

Boundary Conditions

Momentum

B-D (inlet boundary): velocity, $u = u_{a\,in}$
A-C (outlet boundary): pressure, $P = P_{atm}$
A-B and C-D (walls): No slip conditions

Heat transfer

E-G, G-H, and H-F: Thermal insulation
E-F: temperature, $T = T_w$
C-E and D-F: Thermal insulation
C-D: temperature, T = T
A-B: Thermal insulation
B-D: temperature, $T = T_{a\,in}$
A-C: Outflow

Mass transfer

C-E and D-F: No flux
E-F: concentration, $c = c_w = (P_{0w}\, a_w) / (R\, T)$
C-D: concentration, $c = c_a = P_{0a} / (R\, T)$
where P_{0w} and P_{0a} denote the pressure of saturated vapor of hot and cold side, respectively.

Numerical Solution of Governing Equations

The model equations related to feed momentum, heat, and mass transfer with the boundary conditions were solved using COMSOL Multiphysics® version 5 software. The latter uses finite element method analysis and a mesh consisting of 32486 elements for numerical solution of the governing equations developed in this work. A system with the specifications of Intel® CoreTM i5-4210U CPU @ 1.70GHz 2.40 GHz and 6 GB RAM was used to solve the equations.

RESULTS AND DISCUSSION

With the model, parametric studies can be done. Simulations are performed to investigate the effects of various membrane parameters and operating conditions on system performance. The effect of water and air temperatures, air velocity, membrane porosity, pore size, and membrane thickness on the magnitude of molecular flux and $\Delta W/\Delta h$ was investigated. The latter ratio predicts the "moisture-enthalpy ratio". It may be estimated as the difference in humidity ratio (g of water vapor/ kg of dry air) between outlet and inlet air channel boundaries to the difference in enthalpy (kJ/kg) between the same boundaries.

Effect of Water and Air Temperatures on the Molecular Flux

Since the driving force in the membrane distillation process is the temperature difference between two contacting phases, the temperature effect in the SGMD is of great importance. Fig.3 shows the values of MD molecular flux as a function of the seawater temperature for different values of air inlet temperature. It can be seen that the flux increases with water temperature. This increase may be explained by the increase in the water vapor pressure difference, according to the exponential relation between water vapor pressure and temperature predicted by the Antoine equation. On the other hand, for a specified water temperature, a decrease in the molecular flux with sweeping air temperature can be observed. This trend is not unexpected if one considers that an increase in the sweeping air temperature means an increase in the cold temperature, and consequently, a decrease in the thermally induced vapor pressure gradient, which is the driving force for the MD process. Also, it can be noticed that the molecular flux is more affected by the change of water temperature than that of air temperature. For air temperature of 20 ^{0}C, the increase of water temperature by 20 ^{0}C (from 50 to 70 ^{0}C) increases the flux by 200% while at water temperature of 60 ^{0}C, the decrease of air temperature by 20 ^{0}C (from 40 to 20 ^{0}C) increases the flux by only 40%. In other words, at constant temperature difference between the hot and the cold fluid, the permeate flux increases when the temperature of the hot fluid rises. This result is in agreement with Abdullah Alkhudhiri et. al. [4] who stated that the permeate flux is more dependent of the hot fluid temperature.

Effect of Water and Air Temperatures on the Moisture-Enthalpy Ratio

The variation of $\Delta W/\Delta h$ with seawater temperature was investigated and plotted in Fig. 4. There is an increase for $\Delta W/\Delta h$ with both water and air temperatures. So, according to the present simulation, a maximum magnitude was recorded with water and air temperatures of 70 and 40 ^{0}C, respectively. The humidity ratio is sensitive to any change of temperature for both sides.

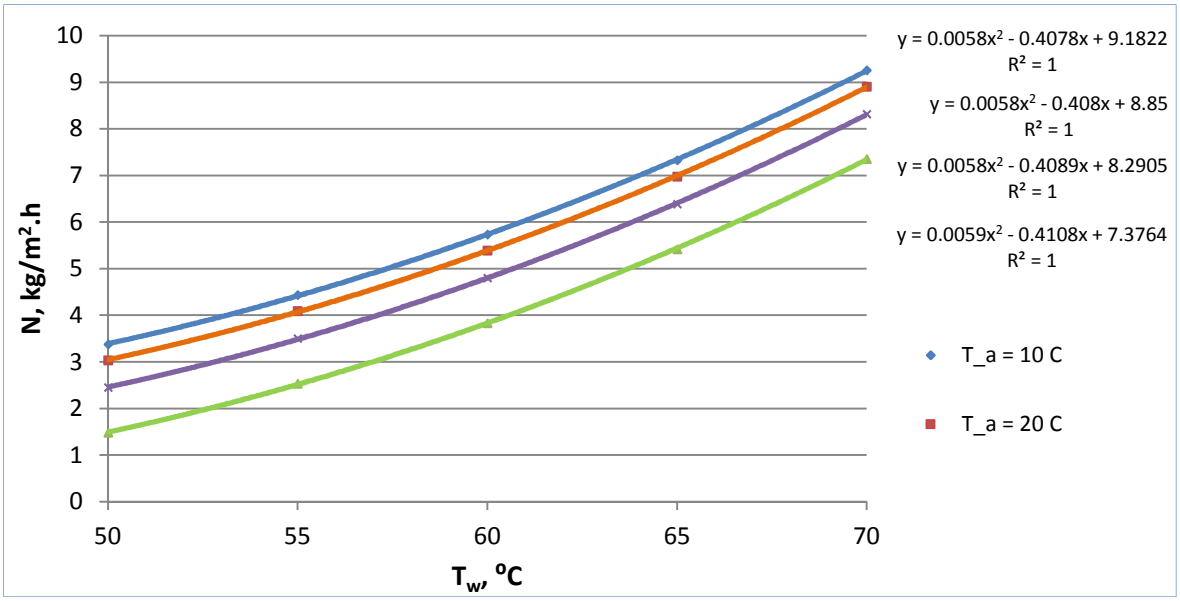

Figure 3. Effect of water and air temperatures on the molecular flux.

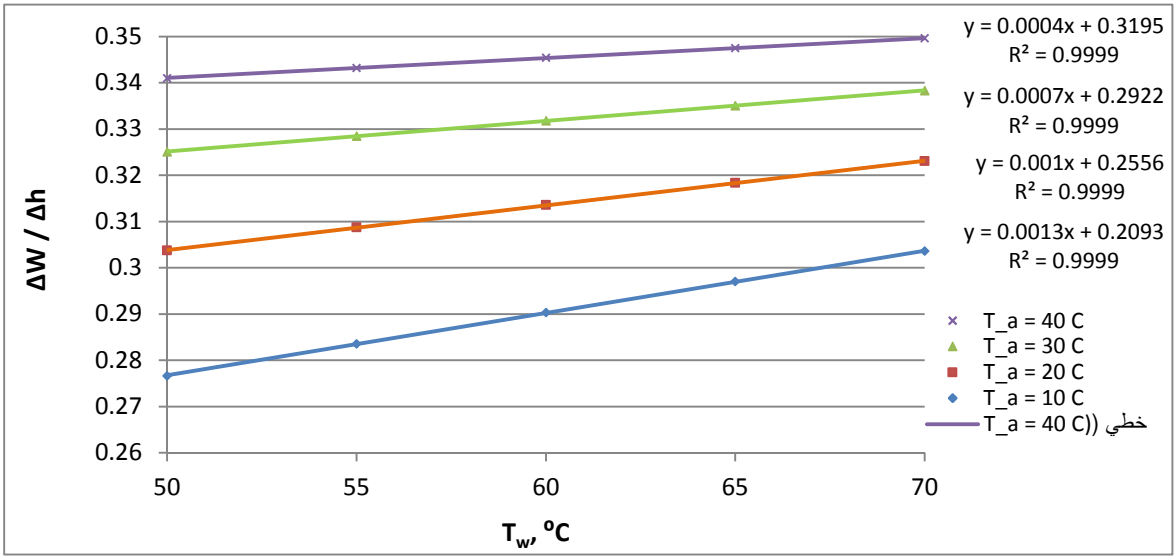

Figure 4. Effect of water and air temperatures on the moisture-enthalpy ratio.

Effect of Air Velocity on the Molecular Flux

As it is illustrated in Fig. 5, the higher air inlet velocity the higher the molecular flux but with different sensitivities dependent on the water temperature. As the air velocity changes from 0.2 to 3 m/s, the molecular flux increases by about 17% regardless the water temperature. As the air velocity increases, the thickness of mass transfer boundary layer decreases, giving rise to flux increase. It is also observed that no significant change in flux for air velocities more than 1.4 m/s.

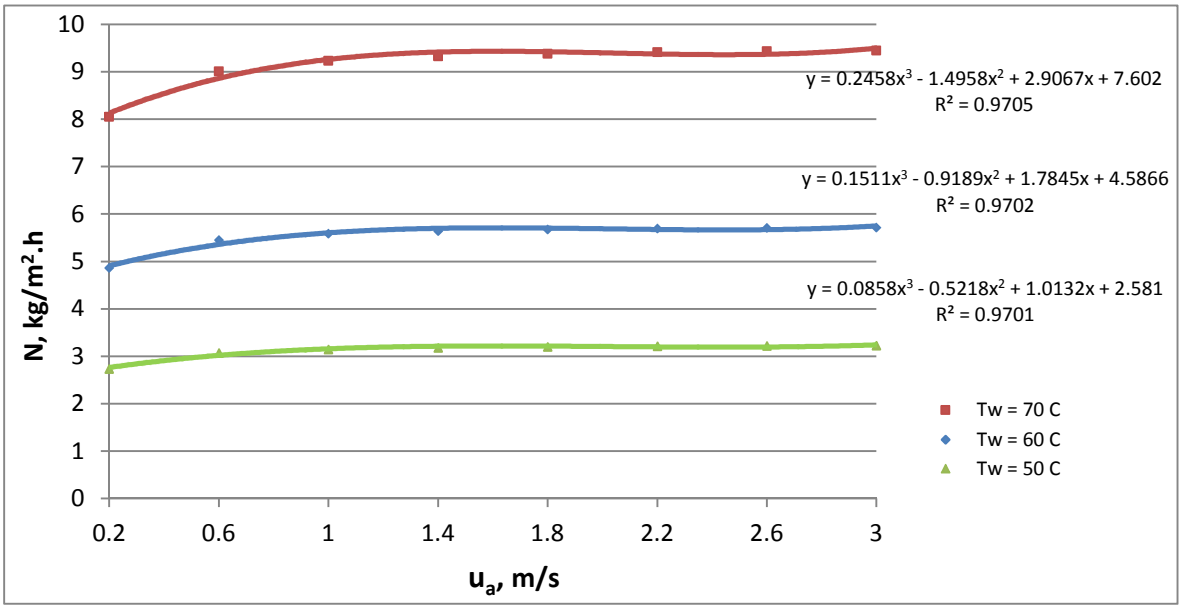

Figure 5. Effect of air velocity on the molecular flux.

Effect of Air Velocity on the Moisture-Enthalpy Ratio

In respect of ΔW/Δh, Fig. 6 shows no significant changes were recorded where the highest recorded variation was 7% at water temperature of 70 ^{0}C.

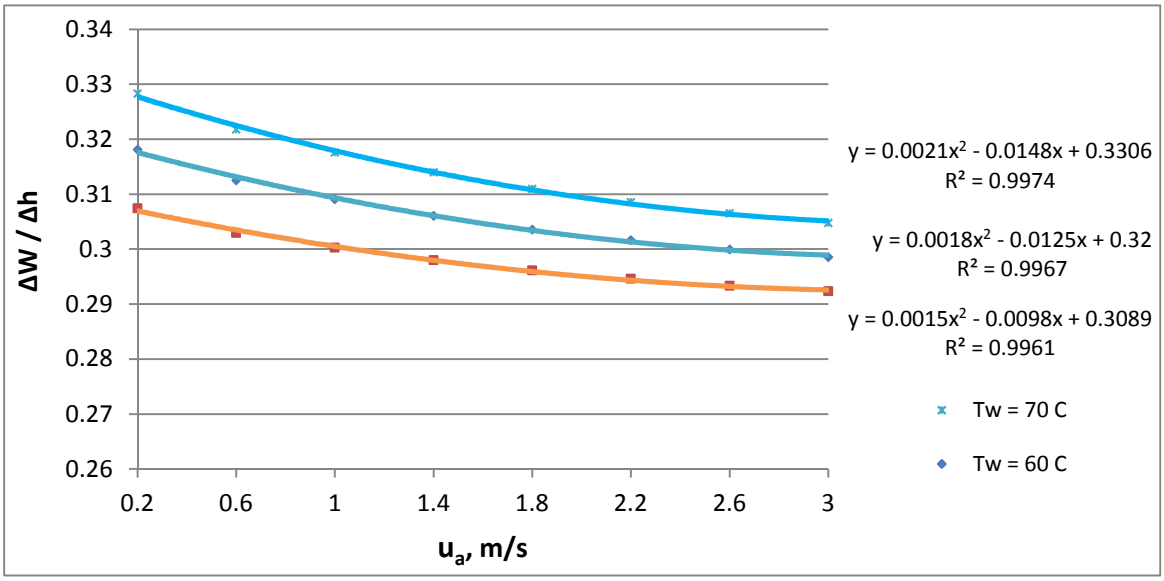

Figure 6. Effect of air velocity on the moisture-enthalpy ratio.

Effect of Membrane Porosity on the Molecular Flux

For membranes, porosity is one parameter that characterizes membrane performance. This character is reflected in Fig. 7, which shows the effect of membrane porosity on the molecular flux. The flux increases linearly with the porosity increase. The higher porosity means greater volume of voids to the total volume of membrane and hence less membrane resistance. Membranes with high porosity are beneficial for performance improvement from the point of view of both mass and heat transfer. Presence of voids decreases heat transfer by conduction which considered as a heat loss in MD process.

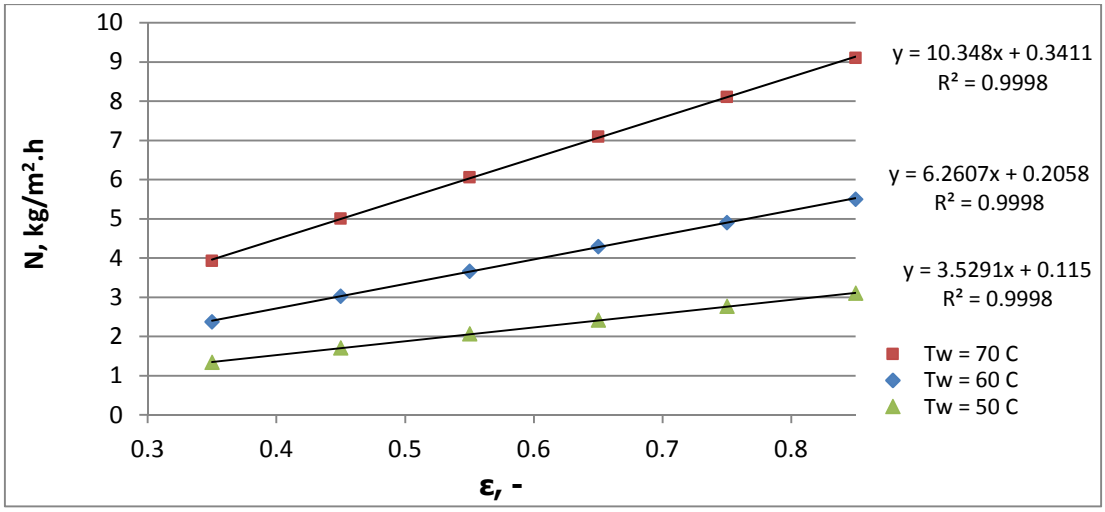

Figure 7. Effect of porosity on the molecular flux.

Effect of Pore Diameter on the Molecular Flux

Besides membrane porosity, mean pore diameter is another important parameter that dictates membrane performance. This is in accordance with our observations from Fig. 8. By increasing the pore diameter from 100 to 450 nm, the molecular flux increases by about 79, 81, 83% at water temperatures 50, 60, and 70 ^{0}C, respectively. Generally, larger pore diameters are better for moisture diffusion, as long as liquid solution does not penetrate into pores [19].

For given experimental conditions [15], the calculated DCMD flux considering Knudsen mechanism is higher than that considering the combined Knudsen/molecular diffusion mechanism. As a consequence, it is advisable to choose the appropriate pore size taking into account the value of the mean free path of the transported molecules from the feed solution and trying to drive the membrane to work under Knudsen type of flow [20].

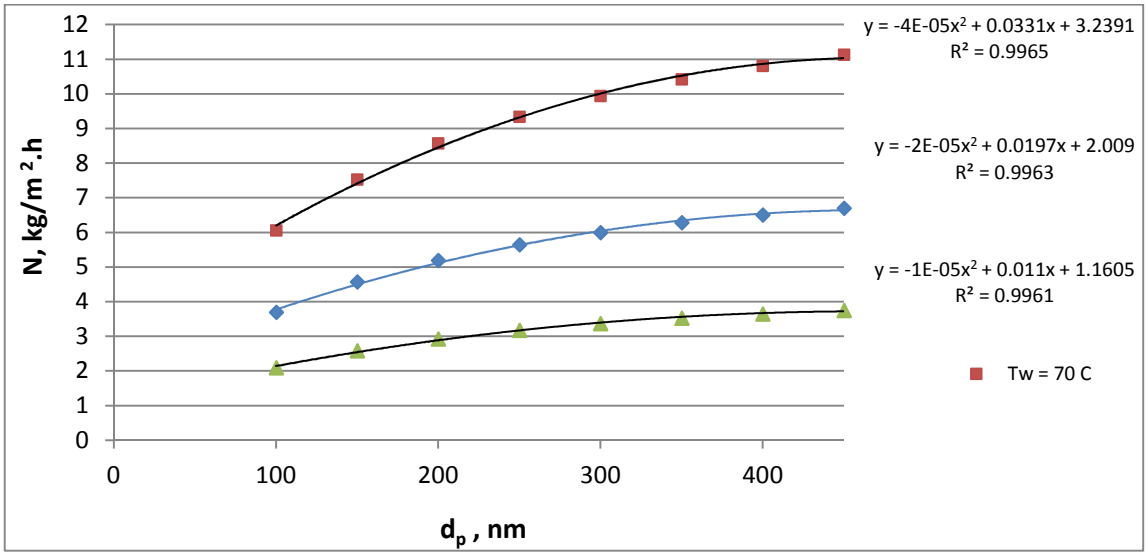

Figure 8. Effect of pore diameter on the molecular flux.

Effect of Membrane Thickness on the Molecular Flux

From Figure 9, the molecular flux declined rapidly when the membrane thickness was increased, as expected from the inverse proportional relationship between N and δ. For the three water temperatures studied, the flux dropped by about 77% when the membrane thickness increased from 0.4 to 2 mm. However, it is worthy here to point out the dual significant role of membrane thickness. To obtain a high MD permeability, the membrane should be as thin as possible. On the contrary, to achieve better heat efficiency, the membrane should be as thick as possible due to the fact that in MD heat loss by conduction takes place through the membrane matrix.

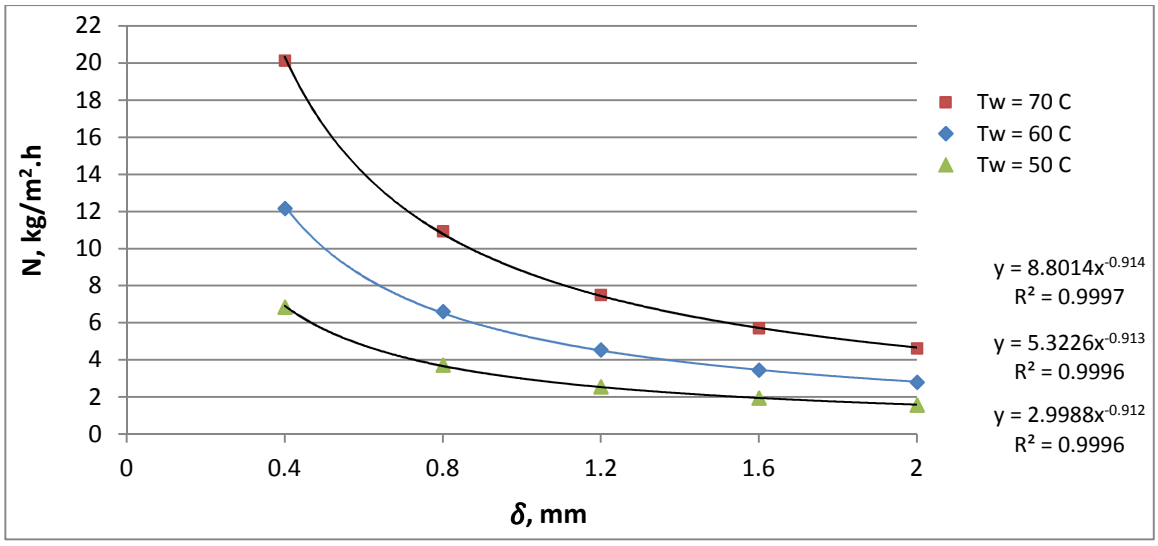

Figure 9. Effect of membrane thickness on the molecular flux.

CONCLUSIONS

A two-dimensional mathematical model is developed to predict the mass transport operation of water using a flat-sheet membrane contactor as sweeping gas membrane distillation (SGMD). CFD simulation was carried out to investigate the influence of water and air temperatures, air velocity, membrane porosity, pore size, and membrane thickness on the molecular flux of water through the membrane and the moisture-enthalpy ratio. The basic equations of transport including momentum, heat, and mass were solved numerically by using COMSOL Multiphysics® software which uses finite element method to perform the simulation. The model was firstly verified through comparing with theoretical data reported in literature. The simulation results revealed that the temperature of the liquid feed and the velocity of the sweeping gas were the most important effective parameters. The membrane characteristics; namely porosity, pore size, and thickness have an important role in the molecular diffusion process.

REFERENCES

[1] Efrem Curcio and Enrico Drioli, Separation and Purification Reviews, Membrane Distillation and Related Operations—A Review, 2005, 34: 35–86, DOI: 10.1081/SPM-200054951.

[2] T Humplik, J Lee, S CO'Hern, B A Fellman, M A Baig, S F Hassan, M A Atieh, F Rahman, T Laoui, R Karnik, ENWang, Nanotechnology, Nanostructured materials for water desalination, 2011, 22: 292001 (19pp), DOI:10.1088/0957-4484/22/29/292001.

[3] Izquierdo-Gil, María Amparo, Cristóbal Fernández-Pineda, and M. G. Lorenz., Journal of Membrane Science, Flow rate influence on direct contact membrane distillation experiments: different empirical correlations for Nusselt number, 2005, 321.2: 356-363, DOI:10.1016/j.memsci.2008.05.018.

[4] Abdullah Alkhudhiri, Naif Darwish, Nidal Hilal, Desalination, Membrane distillation: A comprehensive review, 2012, 287: 2–18, DOI:10.1016/j.desal.2011.08.027.

[5] M. Khayet, C. Cojocaru, A. Baroudi, Desalination, Modeling and optimization of sweeping gas membrane distillation, 2012, 287: 159–166, DOI:10.1016/j.desal.2011.04.070.

[6] M. Khayet, M.P. Godino, J.I. Mengual, Desalination, Theoretical and experimental studies on desalination using the sweeping gas membrane distillation method, 2003, 157: 297-305.

[7] Mehdi Ghadiri, Safoora Fakhri, Saeed Shirazian, Polymer Engineering And Science, Modeling of Water Transport Through Nanopores of Membranes in Direct-Contact Membrane Distillation Process, 2013, DOI 10.1002/pen.23601.

[8] Hui Yu, Xing Yang, Rong Wang, Anthony G. Fanea, Journal of Membrane Science, Analysis of heat and mass transfer by CFD for performance enhancement in direct contact membrane distillation, 2012, 405– 406: 38–47, DOI:10.1016/j.memsci.2012.02.035.

[9] Saeed Shirazian, Seyed N. Ashrafizadeh, Chem. Eng. Technol., 3D Modeling and Simulation of Mass Transfer in Vapor Transport through Porous Membranes, 2013, 36 (1): 177–185, DOI: 10.1002/ceat.201200299.

[10] Saeed Shirazian, Abdolreza Moghadassi, Sadegh Moradi, Simulation Modelling Practice and Theory, Numerical simulation of mass transfer in gas–liquid hollow fiber membrane contactors for laminar flow conditions, 2009, 17:708–718, DOI:10.1016/j.simpat.2008.12.002

[11] M. H. Al-Marzouqi, M. H. El-Naas, S. A. M. Marzouk, M. A. Al-Zarooni, Nadia Abdullatif, Rami Faiz, Separation and Purification Technology, Modeling of CO2 absorption in membrane contactors, 2008, 59: 286–293, DOI:10.1016/j.seppur.2007.06.020.

[12] Mehdi Ghadiri, Safoora Fakhri, Saeed Shirazian, Industrial & Eng. Chem. Res., Modeling and CFD Simulation of Water Desalination Using Nanoporous Membrane Contactors, 2013, 52: 3490–3498, DOI:10.1021/ie400188q.

[13] Tsung-Ching Chen, Chii-Dong Ho, Ho-Ming Yeh, Journal of Membrane Science, Theoretical modeling and experimental analysis of direct contact membrane distillation, 2009, 330: 279–287, DOI:10.1016/j.memsci.2008.12.063.

[14] K. W. Lawson, D. R. Lloyd, J. Membr. Sci., Membrane distillation, 1997, 124 (1), 1–25.

[15] Mohamed Khayet, Paz Godino, Juan I. Mengual, Journal of Membrane Science, Nature of flow on sweeping gas membrane distillation, 2000, 170: 243–255.

[16] W. He, W. Lv, J. Dickerson, SpringerBriefs in Energy, Gas Transport in Solid Oxide Fuel Cells, Chapter 2, 2014, ISBN: 978-3-319-09736-7, DOI: 10.1007/978-3-319-09737-4_2.

[17] S. Al-Obaidani, et al., J. Membr. Sci., Potential of membrane distillation in seawater desalination: thermal efficiency, sensitivity study and cost estimation, 2008, 323 (1): 85–98, doi:10.1016/j.memsci.2008.06.006.

[18] I. Hitsov, T. Maere, K. De Sitter, C. Dotremont, I. Nopens, Separation and Purification Technology, Modelling approaches in membrane distillation: A critical review, 2015, 142: 48–64, DOI:10.1016/j.seppur.2014.12.026.

[19] Li-Zhi Zhang, Separation Science and Technology, Mass Diffusion in a Hydrophobic Membrane Humidification/Dehumidification Process: the Effects of Membrane Characteristics, 2006, 41: 1565–1582, DOI: 10.1080/01496390600634723.

[20] Mohamed Khayet, Advances in Colloid and Interface Science, Membranes and theoretical modeling of membrane distillation: A review, 2011, 164: 56–88, DOI:10.1016/j.cis.2010.09.005.

APPENDIX A

Verification of the Developed Model

The used parameters was as follows: temperatures of 60 ^{0}C and 20 ^{0}C for feed and permeate fluids, respectively; flow rate of 7.5e-5 m3/s for both sides; channel thickness of 1 mm for both sides; membrane material of PTFE with length 40 cm, thickness 0.1 mm, porosity 0.83, and pore diameter 220 nm [13]. A combination of the Knudsen flow and Poiseuille flow was used in the model for estimation of diffusion inside the membrane pores. The model equations were solved using COMSOL Multiphysics® version 3.5.

A.1 Comparison of temperature profile (x-direction) between present results and previous results [12]:

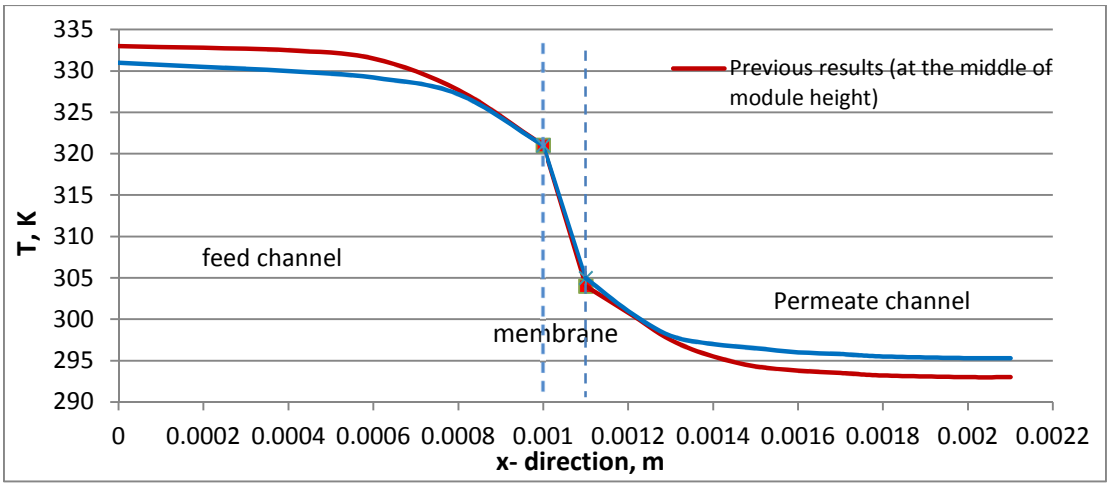

A.2 Comparison of temperature profile (y-direction) between present results and previous results [7]:

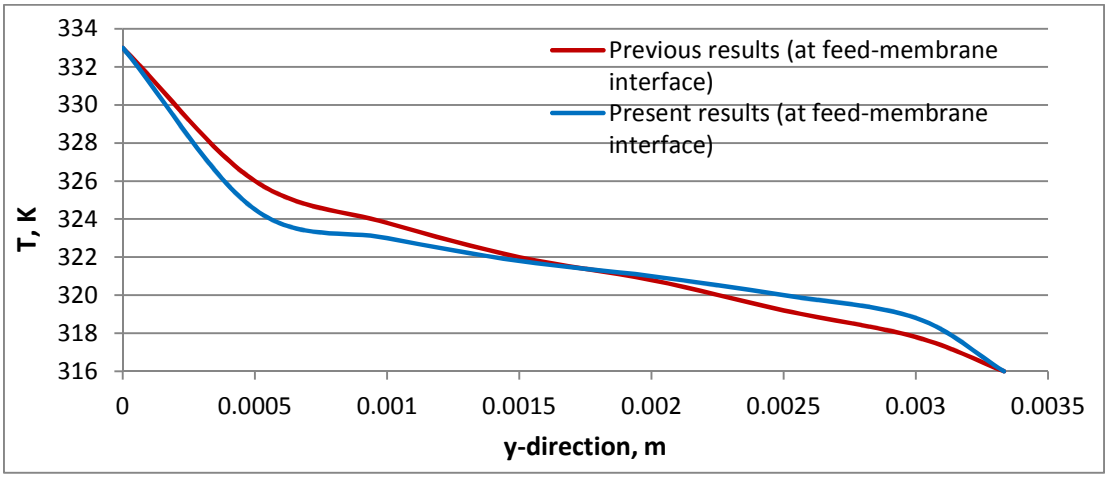

A.3 Comparison of water vapor molecular flux between present results and previous results [7].

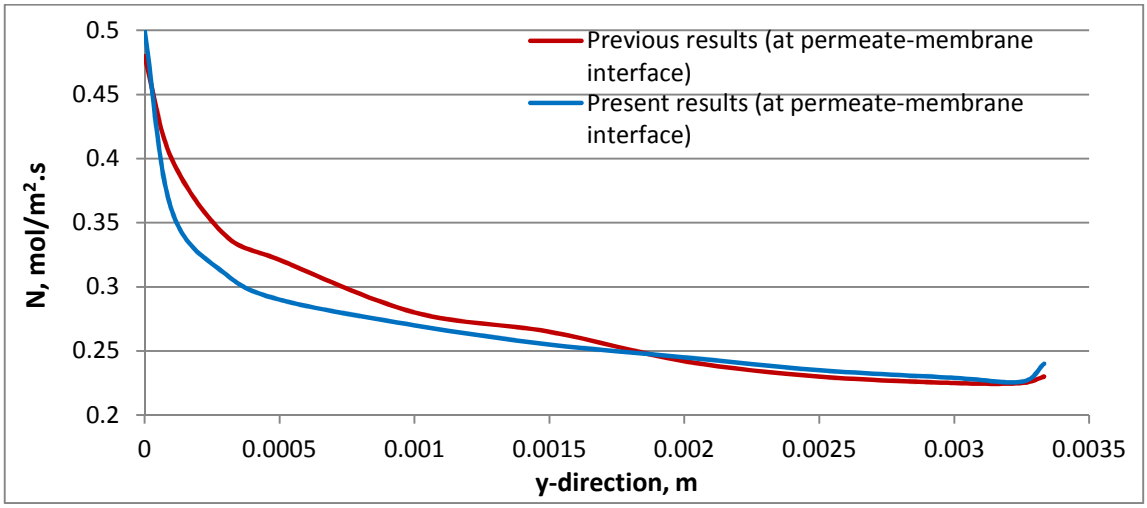

A.4 Comparison of the concentration profile between present results and previous results [12].

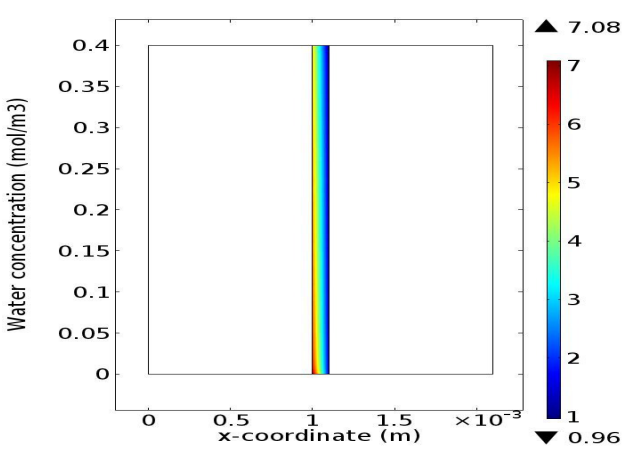

Present results

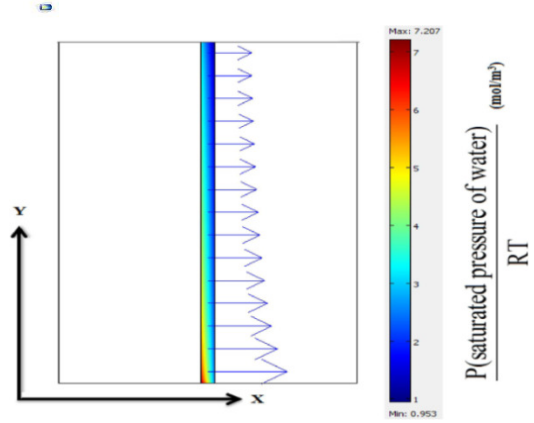

Previous results [12]